Table III—Effect of Theophylline on Net Water Flux from Small Intestine of Rats in Presence of Sørensen's Buffer, Propylene Glycol Solution, and Glycerin Solution

Additive	Net Water Flux, ml/cm/20 min × 10^2	
	Theophylline Present[a]	Theophylline Absent[b]
None	0.95 ± 0.15	0.90 ± 0.25
0.1 *M* propylene glycol	4.30 ± 0.35	4.45 ± 0.40
1 *M* propylene glycol	4.45 ± 0.70	4.55 ± 0.65
0.1 *M* glycerin	3.65 ± 0.30	3.50 ± 0.35
1 *M* glycerin	1.60 ± 0.45	1.80 ± 0.50

[a] Mean of four animals ± *SD*; initial theophylline concentration of 50 mg/100 ml. [b] Mean of three animals ± *SD*. None of these values differed significantly ($p > 0.6$) from those in the presence of theophylline.

tionship between these two effects. The mechanism of the absorption enhancing effect of the alcohols is still being investigated in this laboratory. The magnitude of the effect of propylene glycol and glycerin on the net water flux was not affected by the presence of theophylline, nor did theophylline affect the net water flux from alcohol-free solutions (Table III).

The results of the present study show that the absorption enhancing effect of ethanol on theophylline is not specific to that alcohol. It is shared by propylene glycol and glycerin and, most likely, by other alcohols that were found to increase the net water flux from the intestine. Some of the compounds studied are suitable (and are used widely) as components of pharmaceutical formulations. The fact that they act in very low concentration is particularly striking. Their potential for enhancing the absorption of certain drugs under clinical conditions remains to be explored.

REFERENCES

(1) R. Koysooko and G. Levy, *J. Pharm. Sci.*, **63**, 829(1974).

(2) J. T. Doluisio, N. F. Billups, L. W. Dittert, E. T. Sugita, and J. V. Swintosky, *ibid.*, **58**, 1196(1969).

(3) W. L. Hayton and G. Levy, *ibid.*, **61**, 362(1972).

(4) J. A. Schack and S. H. Waxler, *J. Pharmacol. Exp. Ther.*, **97**, 283(1949).

ACKNOWLEDGMENTS AND ADDRESSES

Received July 29, 1974, from the *Department of Pharmaceutics, School of Pharmacy, State University of New York at Buffalo, Buffalo, NY 14214*

Accepted for publication October 8, 1974.

Supported in part by Grant GM 20852 from the National Institute of General Medical Sciences, National Institutes of Health, Bethesda, MD 20014

[x] To whom inquiries should be directed.

Convective Diffusion Model for a Transport-Controlled Dissolution Rate Process

KENNETH G. NELSON * **and ASHOK C. SHAH** [x]

Abstract □ A mathematical model based on convective diffusion was developed to describe the rate of dissolution from the surface of a compressed compact. Experimental studies were carried out to test the model. The basic experimental apparatus consisted of a modified rotating-filter–stationary basket dissolution test apparatus. Dissolution rates from rectangular and circular surfaces of an homologous series of *p*-aminobenzoate esters permitted testing the theory with respect to solubility, geometry, and agitation conditions. The correlation between experimental results and theory was reasonably good considering that the test conditions were somewhat less than ideal.

Keyphrases □ Diffusion model, convective—transport-controlled dissolution rate process, *p*-aminobenzoates and modified rotating-filter–stationary basket apparatus □ Dissolution rate, transport controlled—convective mathematical diffusion model tested using *p*-aminobenzoates and modified rotating-filter–stationary basket apparatus □ Transport—as controlling factor in dissolution rate process, convective mathematical diffusion model proposed and tested

Reviews of the literature concerning dissolution rates of drugs (1–3) indicate that the most widely accepted theory for dissolution rates is that proposed by Noyes and Whitney in 1897 and subsequently modified to include the stagnant or unstirred diffusion layer concept of Nernst and Brünner[1]. In this form, the rate expression is:

$$\frac{dc}{dt} = \frac{AD}{hv}(c_0 - c) \qquad \text{(Eq. 1)}$$

(The notation is defined at the end of the text.)

It can be seen that the rate is directly proportional to the area exposed, the diffusivity, and the solubility and inversely proportional to the diffusion layer thickness. The first three variables enumerated can be determined by independent measurements, whereas the effective diffusion layer thickness, h, is a model-dependent parameter. As such, its significance and utility outside the confines of the model are necessarily limited.

Transport-controlled dissolution in a stirred liquid involves two fundamental processes: molecular diffusion and forced convection as a result of fluid flow. Although hydrodynamic factors have been discussed and considered to some extent, particularly in regard to the rotating-disk technique (4, 5), a rather general

[1] See review articles for appropriate references.

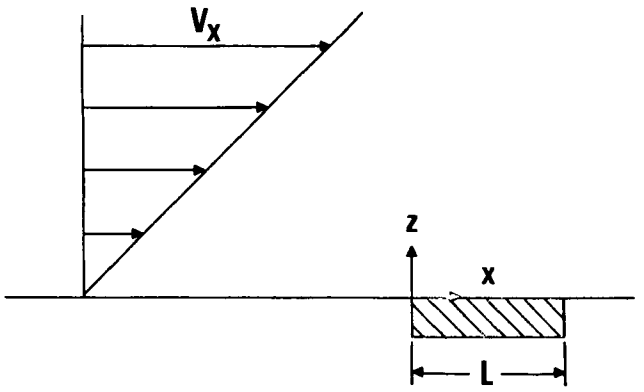

Figure 1—*Convective diffusion model.*

treatment of drug dissolution in terms of diffusion and concomitant convection has not been developed. The purposes of this study were to apply a convective diffusion model to the drug dissolution process and to test the model experimentally.

THEORETICAL

The model to be developed is based on convective diffusion theory, *i.e.*, the mathematical expressions for mass transport by diffusion and convection are combined to give a "convective diffusion" differential equation. The development of an expression for the dissolution rate, then, involves selecting appropriate boundary conditions and solving the differential equation utilizing these boundary conditions.

The convective diffusion equation was given by Levich (6) as:

$$\frac{\partial c}{\partial t} = D \text{ div grad } c - \mathbf{V} \text{ grad } c \qquad \text{(Eq. 2)}$$

The first term on the right side is the diffusion contribution, whereas the second term arises from convection. For steady state, the change in concentration with time is zero, so the steady-state convective diffusion equation is:

$$D \text{ div grad } c = \mathbf{V} \text{ grad } c \qquad \text{(Eq. 3)}$$

The physical model will be developed on the basis of the following assumptions. The liquid is flowing past the dissolving surface in the x direction, and convective flow in the y and z directions is nonexistent. The solid is dissolving by diffusion in the z direction, which is normal to the surface of the dissolving solid. With these assumptions, Eq. 3 becomes:

$$D\frac{\partial^2 c}{\partial z^2} = \mathbf{V}_x \frac{\partial c}{\partial x} \qquad \text{(Eq. 4)}$$

The liquid into which the diffusion occurs requires special consideration. In cases where a solid plane is positioned parallel to unidirectional, frictionless flow, a parabolic laminar hydrodynamic boundary layer develops on the solid (7). If the solid undergoes dissolution, the diffusion boundary layer is also well characterized (7). The flow regime in most equipment designed for drug dissolution tests, however, is turbulent to ensure efficient mixing, so the parabolic boundary layers do not develop. Under certain turbulent circumstances, however, it is customary to consider the fluid layer immediately adjacent to a solid wall as having a laminar nature (8). Thus, it will be assumed that the boundary layer into which the dissolution is occurring is laminar and, furthermore, that it may be described by a linear velocity profile. The liquid velocity term then is given by:

$$\mathbf{V}_x = \alpha z \qquad \text{(Eq. 5)}$$

The physical model is shown in Fig. 1. Substituting Eq. 5 into Eq. 4 yields:

$$D\frac{\partial^2 c}{\partial z^2} = \alpha z \frac{\partial c}{\partial x} \qquad \text{(Eq. 6)}$$

and the boundary conditions are:

$$c = c_0 \quad \text{for } 0 < x < L, \quad z = 0 \qquad \text{(Eq. 7a)}$$
$$c = 0 \quad \text{for } z = \infty \qquad \text{(Eq. 7b)}$$
$$c = 0 \quad \text{for } x = 0 \qquad \text{(Eq. 7c)}$$

The first boundary value requires that a saturated layer always exists at the solid–liquid interface and that any interfacial barrier or reaction is insignificant. The second and third boundary conditions relate to "sink" conditions.

The mathematical solution to Eq. 6 has been presented for an analogous situation (8). It is:

$$c = \frac{c_0\beta\int_{\beta}^{\infty} e^{-\beta^3}\,d\beta}{\Gamma(4/3)} \qquad \text{(Eq. 8a)}$$

$$\beta = z\left(\frac{\alpha}{9Dx}\right)^{1/3} \qquad \text{(Eq. 8b)}$$

Hence, the initial rate of dissolution is:

$$R = -D\left(\frac{\partial c}{\partial z}\right)_{z=0} \qquad \text{(Eq. 9)}$$

If Eq. 8a is substituted into Eq. 9 and the necessary differentiation is performed, Eq. 9 can be integrated over one surface of a rectangular tablet of length L (in the direction of flow) and width b to obtain:

$$R = 0.808 D^{2/3} c_0 \alpha^{1/3} b L^{2/3} \qquad \text{(Eq. 10)}$$

If Eq. 9 is integrated over one surface of a circular tablet of radius r:

$$R = 2.157 D^{2/3} c_0 \alpha^{1/3} r^{5/3} \qquad \text{(Eq. 11)}$$

Equations 10 and 11 should describe the initial dissolution rates from a surface of a rectangular tablet and a disk, respectively, provided that the boundary conditions are met and the assumptions in their derivations are valid.

EXPERIMENTAL

The dissolution rates were determined in a modified rotating-filter–stationary basket apparatus[2] which has been described previously (9, 10). In place of the stationary basket, however, a stainless steel die and holder assembly was developed that would permit the dissolution from a constant area surface of a rectangular nondisintegrating tablet (Fig. 2). The face of the die measured 4.76 × 4.76 cm and was 0.95 cm thick. The edges were beveled at 45° to promote the development of an adherent, laminar boundary layer. The opening for the tablet was 2.54 × 0.317 cm, which gives a length to width ratio of 8:1, and the die could be mounted with either the long or short dimension parallel to the direction of liquid flow. Each tablet was prepared by placing the die face down on a smooth surface, pouring the powder in the opening from the back side, and compressing with an appropriately sized rectangular punch on a hydraulic press[3].

To determine dissolution rates from circular surfaces, a clear plastic die was fabricated having the same external dimensions as the die already described. In place of the rectangular opening, a circular channel of diameter 2.22 cm was bored through the die. Therefore, a flat-faced tablet could be mounted by placing the die face down on a microscope slide and holding the tablet against the slide in the die opening with a probe while pouring molten wax in

[2] Coffman Industries, Kansas City, KS 66101
[3] Carver laboratory press, Fred S. Carver, Inc., Summit, N.J.

Table I—Effect of Die Orientation on the Dissolution Rate (R) of Ethyl p-Aminobenzoates

Revolutions per Minute	Die Orientation		Ratio
	Vertical	Horizontal	
	R, moles min^{-1}		
200	1.274×10^{-6}	8.69×10^{-7}	1.46
300	1.456×10^{-6}	9.19×10^{-7}	1.58
400	1.628×10^{-6}	1.081×10^{-7}	1.51

the opening. This arrangement would accommodate any flat-faced tablet having a diameter less than 2 cm and would ensure that the dissolving surface would be coplanar with the surface of the die.

The positioning of the die in the dissolution apparatus is a critical factor in the development of the flow pattern past the die. To ensure reproducibility and to prevent the boundary layer from separating from the die in the region of the dissolving surface, the following placement was chosen: 4.12 cm from the center of the die holder rod to the center of the rotating filter, 112° angle between the face of the die and an imaginary line connecting the midpoints of the centers of the rotating filter and the die holder and facing into the counterclockwise motion of the liquid, and 12 cm from the upper edge of the die to the lower surface of the apparatus cover. A line mark ascribed on the flask surface (Fig. 2) facilitated accurate positioning of the die. This placement was chosen by subjective evaluation of the behavior of the boundary layer at various orientations of the die in the apparatus. This behavior was observed by utilizing a tablet composed of a water-soluble dye and polyethylene glycol 6000.

The compounds selected for study were the methyl through pentyl esters of p-aminobenzoic acid, which have been well characterized (11). For a typical experiment utilizing the metal die, 200 mg of solid was compressed at 1500 lb for 1 min and the die was held above the water level in the flask until the temperature of the water (1006 ml) and the apparatus was 37°. The die was then positioned as described, and the chart recorder was started for monitoring the ester concentration with a flow cell in a spectrophotometer[4]. The molar absorptivity for these compounds is 1.652×10^4 at 285 nm.

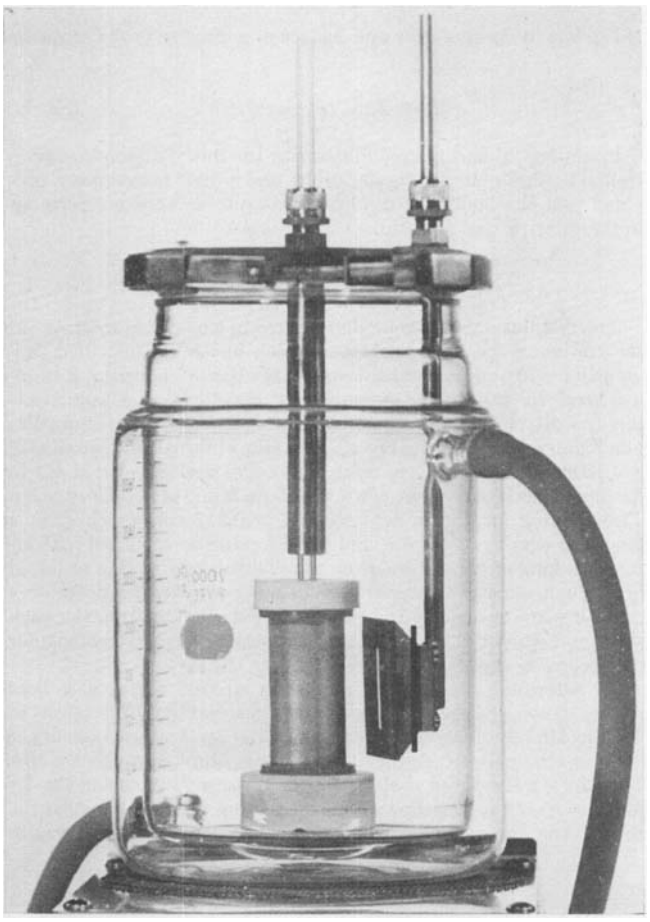

Figure 2—*Dissolution test apparatus.*

Table II—Comparison of Convective Diffusion and Unstirred Layer Theories

Parameter	Unstirred Layer	Convective Diffusion
Solubility	C_0	C_0
Surface (rectangle)	bL	$bL^{2/3}$
Surface (disk)	r^2	$r^{5/3}$
Diffusivity	D	$D^{2/3}$
Shear rate	—	$\alpha^{1/3}$

RESULTS AND DISCUSSION

The convective diffusion dissolution rate expressions (Eqs. 10 and 11) were derived assuming that the boundary layer flows past the dissolving surface in a regular manner. There may be experimental problems in meeting this requirement, however, because the dissolving surface is planar whereas the rotating-filter apparatus produces a tangential annular flow system. When using blue dye as a flow visualization technique, it was observed that the boundary layer flowed along the surface to a point about 0.5 cm forward of the trailing edge of the die, where it separated from the surface and entered the mainstream of flow. Thus, the boundary layer adhered over the dissolving surface, although it did tend to move downward from the horizontal by approximately 10°. A somewhat nonuniform blue density suggested that the boundary layer is affected by eddies entering from the main flow stream. It is expected that these phenomena will reduce the correlation between theory and experiment.

The dissolution rates for the methyl through pentyl esters of p-aminobenzoic acid were determined to test the effect of solubility. According to Eq. 10, the rate is directly proportional to solubility if all other variables remain constant. The rates were determined with the die in the vertical position and a stirring rate of 300 rpm. The solubility values were obtained from Yalkowsky *et al.* (11). Figure 3 is a plot of log R *versus* log c_0, on which a line of slope 1 was constructed to permit visual correlation with theory. The least-squares slope of this plot is 0.939 with a correlation coefficient of 0.997. The correlation between experiment and theory is

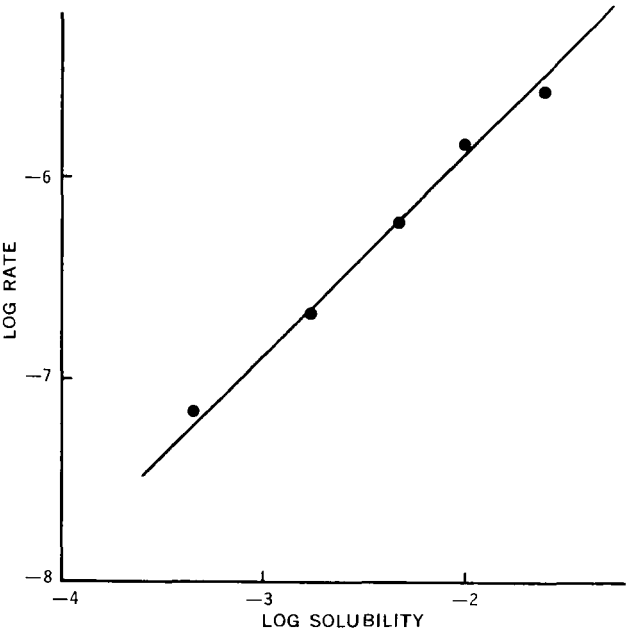

Figure 3—*Log–log plot of rate data as a function of solubility.*

[4] Beckman model DBG, Beckman Instruments, Fullerton, CA 92634

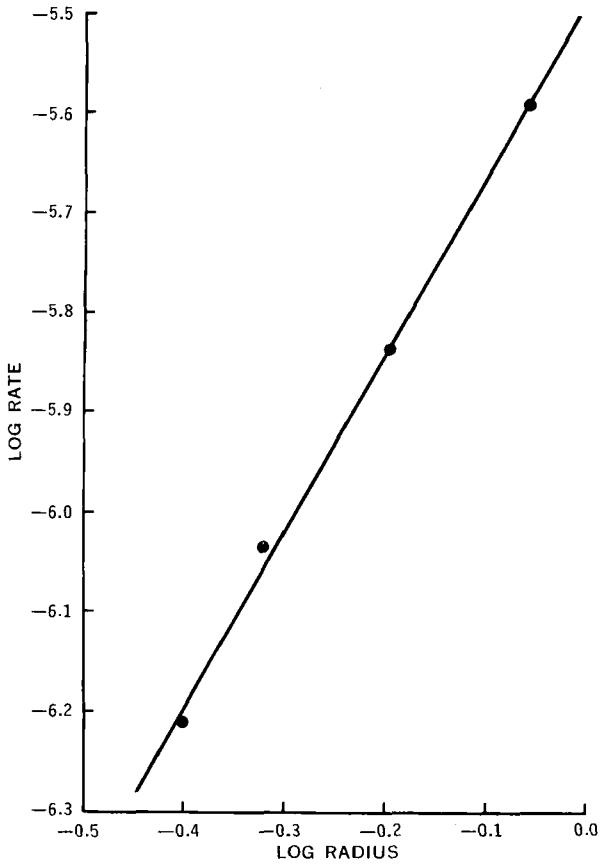

Figure 4—*Log–log plot of rate data as a function of tablet radius.*

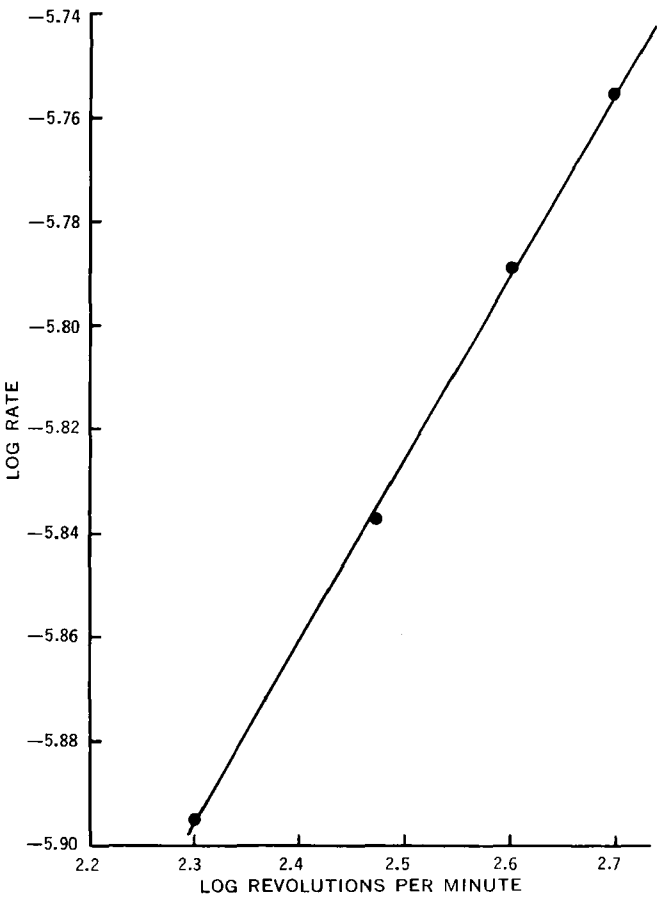

Figure 5—*Log–log plot of rate data as a function of stirring rate.*

good, considering that the diffusivity is changing by a small factor over the ester series and the presence of the more soluble species in the boundary layer may affect the value of α.

The metal die was designed to produce a rectangular tablet with a length to width ratio of 8:1 so that Eq. 10 could be tested with respect to the orientation of the tablet surface relative to the flow. According to Eq. 10, the rate of dissolution should be twice as fast with the tablet in the vertical position, *i.e.*, with the long axis perpendicular to flow, than with the tablet in the horizontal position. Table I shows data obtained using ethyl *p*-aminobenzoate with the die in the two orientations at various stirring rates. While the observed increases of about 50% in the rate in the vertical orientation relative to the horizontal do not indicate the factor of two predicted by Eq. 10, the discrepancy is probably due at least in part to the less than ideal behavior of the boundary layer.

Nevertheless, the observed differences bring out the importance of considering convection along with diffusion. The commonly employed stagnant layer model described by Eq. 1 has the rate directly proportional to area. Since the dissolving surfaces in these experiments have identical areas, Eq. 1 would require stagnant layers of different thicknesses for the two orientations. This is untenable because the flow characteristics for the two orientations are similar.

To test further the rate dependence on surface geometry, dissolution rates were determined for ethyl *p*-aminobenzoate disks mounted in the plastic die. Four tablets were used, ranging from 0.397 to 0.873 cm in radius, with a stirring rate of 200 rpm. A plot of log R *versus* log r is shown in Fig. 4. The least-squares slope of the log–log plot is 1.79, which is closer to the slope of 1.67 expected from convective diffusion theory (Eq. 11) than to 2.00 (from πr^2) in the unstirred layer theory (Eq. 1). Again, while these data are not conclusive, the influence of the convective diffusion phenomenon, *i.e.*, the build-up of solute in the hydrodynamic boundary layer, is apparent.

The one parameter in the convective diffusion theory that cannot be readily measured or calculated independently in this particular experimental system is the rate of shear. The functional dependence on the shear rate can be implicitly evaluated, however, in the following manner. If the rate of shear in the boundary layer is directly proportional to the rate of shear in the bulk liquid, *i.e.*, the stirring rate, then a plot of log R *versus* log revolutions per minute should be a straight line with a slope of 0.33, as required by Eq. 10.

Data for the dissolution rate of ethyl *p*-aminobenzoate from the rectangular die in the vertical orientation as a function of agitation conditions ranging from 200 to 500 rpm are shown as a log–log plot in Fig. 5. A line of slope one-third is drawn through the data according to theory, and the least-squares slope is 0.355 with a correlation coefficient of 0.999. It thus appears that the assumption concerning shear rate in the boundary layer is reasonable under the present conditions. Both the theory and experimental data support the fact that the dissolution rate is a relatively weak function of the stirring rate, *i.e.*, $R \propto \alpha^{1/3}$.

The convective diffusion model presented in this report predicts a dissolution rate having different functional relationships of the variables than the unstirred layer theory. Table II summarizes these dependencies for the two models. It can be seen that the differences lie in the surface area and diffusivity terms. In addition, a hydrodynamic term is present in the convective diffusion theory. Although α might be considered a model-dependent parameter not unlike h, one could design an experimental apparatus in which α would be known *a priori*. This would not be possible for h.

Convective diffusion enables one to describe drug dissolution phenomena on a more realistic basis than prevailing theories. Experimental work is being continued with an apparatus that promotes ideal flow conditions to test the model further.

NOTATIONS

A = area of dissolving surface
b = width of tablet; perpendicular to flow
c = concentration of solute
c_0 = solubility of solute
D = diffusivity of solute

h = effective diffusion layer thickness
L = length of tablet; parallel to flow
r = radius of tablet surface
R = rate of dissolution
t = time
v = volume of solution
$\mathbf{V}$ = vector describing liquid flow
V_x = x component of liquid velocity
x,y,z = cartesian coordinates
α = rate of shear in boundary layer
Γ = gamma function
β = dimensionless variable

REFERENCES

(1) D. E. Wurster and P. W. Taylor, *J. Pharm. Sci.*, **54**, 169(1965).

(2) W. I. Higuchi, *ibid.*, **56**, 315(1967).

(3) J. G. Wagner, *ibid.*, **50**, 359(1961).

(4) P. Singh, S. J. Desai, D. R. Flanagan, A. P. Simonelli, and W. I. Higuchi, *ibid.*, **57**, 959(1968).

(5) G. Levy, *ibid.*, **52**, 1039(1963).

(6) V. Levich, "Physicochemical Hydrodynamics," Prentice-Hall, Englewood Cliffs, N.J., 1962.

(7) H. Schlichting, "Boundary Layer Theory," 6th ed., McGraw-Hill, New York, N.Y., 1968.

(8) R. B. Bird, W. E. Stewart, and E. N. Lightfoot, "Transport Phenomena," Wiley, New York, N.Y., 1960.

(9) A. C. Shah, C. B. Peot, and J. F. Ochs, *J. Pharm. Sci.*, **62**, 671(1973).

(10) A. C. Shah and J. F. Ochs, *ibid.*, **63**, 110(1974).

(11) S. H. Yalkowsky, G. L. Flynn, and T. G. Slunick, *ibid.*, **61**, 852(1972).

ACKNOWLEDGMENTS AND ADDRESSES

Received May 13, 1974, from *Pharmacy Research, The Upjohn Company, Kalamazoo, MI 49001*

Accepted for publication September 26, 1974.

* Present address: College of Pharmacy, University of Minnesota, Minneapolis, MN 55455

‡ To whom inquiries should be directed.

Substituted Thiazolidones: Selective Inhibition of Nicotinamide Adenine Dinucleotide-Dependent Oxidations and Evaluation of Their CNS Activity

SUNIL K. CHAUDHARI *, MAHIMA VERMA *, ARVIND K. CHATURVEDI *, and SURENDRA S. PARMAR *‡x

Abstract □ Eight 2-arylimino-3-(3-*N*-morpholinopropyl)thiazolid-4-ones were synthesized from the corresponding 1-aryl-3-(3-*N*-morpholinopropyl)thiocarbamides, characterized, and tested for their effects on the cellular respiratory activity of rat brain homogenates. All substituted 4-thiazolidones selectively inhibited nicotinamide adenine dinucleotide (NAD)-dependent oxidations of pyruvate, citrate, DL-isocitrate, α-ketoglutarate, malate, β-hydroxybutyrate, L-glutamate, and NADH, while the NAD-independent oxidation of succinate remained unaltered. All thiazolidones possessed some degree of anticonvulsant activity against pentylenetetrazol-induced convulsions, and the protection afforded by these compounds at a dose of 100 mg/kg ranged from 30 to 80%. The low toxicity possessed by most of these thiazolidones was reflected by their approximate LD_{50} values from 300 mg/kg to greater than 1000 mg/kg. In the present study, the anticonvulsant activity possessed by these substituted 4-thiazolidones was unrelated to their ability to inhibit selectively the NAD-dependent oxidations by rat brain homogenates. These thiazolidones exhibited depression of the CNS activity which, in some cases, was associated with the increase in respiration. All thiazolidones potentiated pentobarbital (sodium) sleeping time in mice when administered in a dose of 100 mg/kg.

Keyphrases □ Thiazolidones, 2-arylimino-3-(3-*N*-morpholinopropyl)—synthesis, inhibition of NAD-dependent oxidations and relationship to anticonvulsant activity □ Structure–activity relationships—thiazolidones, anticonvulsant activity, inhibition of NAD-dependent oxidations, rats □ Anticonvulsant activity, thiazolidones—relationship to inhibition of NAD-dependent oxidations

Thiazolidones have been shown to possess diverse biological properties including hypnotic (1), local anesthetic (2), and anticonvulsant (3, 4) activities. Recent studies indicated the anticonvulsant activity of piperazinothiocarbamides (5, 6) and their ability to inhibit nicotinamide adenine dinucleotide (NAD)-dependent oxidations. Furthermore, compounds possessing a morpholino group attached to the heterocyclic nuclei have been shown to confer greater activity and less toxicity (7). These observations led to the synthesis of some 2-arylimino-3-(3-*N*-morpholinopropyl)thiazolid-4-ones and correlation of certain pharmacological properties with their ability to inhibit NAD-dependent oxidations.

EXPERIMENTAL[1]

The various 1,3-disubstituted thiocarbamides were prepared by refluxing an equimolar quantity of 3-*N*-morpholinopropylamine and different arylisothiocyanates in dry benzene. These substituted thiocarbamides, when refluxed with chloroacetic acid and anhydrous sodium acetate in absolute ethanol, formed the desired substituted thiazolidones (8).

1 - Aryl - 3 - (3 - *N* - morpholinopropyl)thiocarbamide—3 - *N* - Morpholinopropylamine (0.01 mole) was mixed with suitable aryl isothiocyanate (0.01 mole) in 15 ml of dry benzene, and the mixture was refluxed on a steam bath for 2 hr. The reaction mixture was concentrated by removing benzene by distillation under reduced pressure. The solid that separated on cooling was filtered, washed with ether and dilute hydrochloric acid, dried, and recrystallized from ethanol. All thiocarbamides were characterized by their sharp melting points and elemental analyses (Table I).

[1] All compounds were analyzed for their carbon, hydrogen, and nitrogen contents. Melting points were taken in open capillary tubes with a partial immersion thermometer and are corrected.